

Relationship between spectral indices and quality parameters of tifton 85 forage

Relação entre índices espectrais e parâmetros de qualidade da forrageira tifton 85

Jhiorranni F. Souza¹, Anderson G. Costa^{1*}, João C. L. de Carvalho¹, Lucas A. dos Santos¹, Vinícius P. Silva²,
Murilo M. de Barros¹

¹Engineering Department, Technology Institute, Universidade Federal Rural do Rio de Janeiro, Seropédica, RJ, Brazil. ²Department of Animal Nutrition and Pastures, Animal Science Institute, Universidade Federal Rural do Rio de Janeiro, Seropédica, RJ, Brazil.

ABSTRACT - Computer vision systems can be an alternative to traditional methods of analyzing the quality of forage crops, allowing the instantaneous, non-destructive monitoring of the crop, with cost reduction. This study aimed to evaluate the quality parameters of Tifton 85 (*Cynodon* spp.) using digital images, relating spectral indices to the quality parameters of this forage. In the experimental area, four levels of nitrogen fertilization were applied and the analyses were made at different times after the standardization cut (14, 28, 42, and 56 days). The quality parameters evaluated were mineral matter, crude protein, and neutral detergent fiber. From images obtained in the visible (RGB) and near-infrared (RGNIR) spectral regions, spectral indices were generated. Principal component analysis was applied to summarize the information obtained by spectral indices into a single principal component (PC1). PC1 associated with spectral indices was related to forage quality parameters for each cutting time using simple quadratic regression models. The relationships between mineral matter and spectral indices were variable over time. Crude protein and neutral detergent fiber showed the highest relationships with the spectral indices obtained by RGNIR images already at the initial times. Thus, although the RGB images have shown satisfactory results to obtain information about the quality of Tifton 85, the NIR band tends to increase the reliability of the relationships at early times.

RESUMO - Sistemas de visão computacional podem ser uma alternativa aos métodos tradicionais de análise de qualidade de culturas forrageiras, permitindo o monitoramento da lavoura de forma instantânea, não destrutiva, e com redução de custos. Esta pesquisa teve como objetivo avaliar parâmetros de qualidade do capim Tifton 85 (*Cynodon* spp.) por meio de imagens digitais, relacionando índices espectrais com parâmetros de qualidade desta forrageira. Na área experimental foram aplicados quatro níveis de adubação nitrogenada e as análises foram realizadas em diferentes épocas após o corte de uniformização (14, 28, 42 e 56 dias). Os parâmetros de qualidade avaliados foram a matéria mineral, proteína bruta e fibra em detergente neutro. A partir de imagens obtidas na região espectral do visível (RGB) e do infravermelho próximo (RGNIR), foram gerados índices espectrais. A análise de componentes principais foi aplicada para condensar as informações obtidas pelos índices espectrais em um único componente principal (PC1). Os PC1 associados aos índices espectrais foram relacionados com os parâmetros de qualidade da forrageira para cada época de corte utilizando modelos de regressão quadrática simples. As relações da matéria mineral e os índices espectrais foram variáveis ao longo das épocas. A proteína bruta e fibra em detergente neutro apresentaram as maiores relações com os índices espectrais obtidos pelas imagens RGNIR já nas épocas iniciais. Assim, embora as imagens RGB tenham apresentado resultados satisfatórios para se obter informações sobre a qualidade do Tifton 85, a utilização da banda NIR tende a aumentar a confiabilidade das relações em instantes de tempo precoces.

Keywords: *Cynodon* spp. Pastures. Computer vision. Digital images.

Palavras-chave: *Cynodon* spp. Pastagens. Visão computacional. Imagens digitais.

Conflict of interest: The authors declare no conflict of interest related to the publication of this manuscript.

INTRODUCTION

The farming market has been proving to be increasingly demanding with the nutritional quality of forage used for animal feed. Searching for technological innovations that make it possible to sustainably increase the productivity and nutritional quality of pastures is essential for the farming sector to remain profitable (AHMAD et al., 2023). According to FAO (2022), Brazil ranks second among the largest beef producers, with a production of approximately 10 million tons, behind the United States. The forage market in Brazil moves more than R\$ 1.4 billion a year, with tropical forage grasses representing the largest part of this market (EMBRAPA, 2021).

Among tropical forages, the genus *Cynodon* has been widely used for intensifying livestock production due to its high nutritional value, biomass production, rapid hay production, and good drought tolerance (SOUZA et al. 2020). Within this genus, Tifton 85 is considered the best hybrid, with good adaptation to tropical and subtropical conditions (SILVA et al., 2020).

Traditional methods for monitoring parameters related to forage quality often require costly, time-consuming laboratory analysis and specialized labor, as is the case with the evaluation of crude protein (WANG et al., 2023), dry matter



This work is licensed under a Creative Commons Attribution-CC-BY <https://creativecommons.org/licenses/by/4.0/>

Received for publication in: August 18, 2023.

Accepted in: January 9, 2024.

***Corresponding author:**

<acosta@ufrj.br>

(SOMAVILLA et al., 2021), and neutral detergent fiber (PETERS et al., 2022).

Spectral indices obtained from digital images have been used with recognized success in the evaluation of biophysical parameters of different crops. In forage crops, the use of digital images has enabled the instantaneous, non-destructive quantification of leaf area and leaf weight (HUACCHA-CASTILLO et al., 2023), nitrogen fertilization estimation (MANCIN et al., 2022), aboveground biomass estimation (MAIMAITIJANG et al., 2019), productivity estimation (SERRET et al., 2020), and chlorophyll monitoring (KRÍŽOVÁ et al., 2022).

In this context, the relationship between the spectral characteristics and the nutritional parameters of the crop should also be evaluated to expand the measurement possibilities from technologies based on digital images. Furthermore, the measurement of nutritional attributes such as mineral matter, crude protein, and neutral detergent fiber using automated systems based on computer vision can represent a complementary alternative to laboratory analysis, allowing instantaneous measurements in loco and increasing the amount of information about the nutritional quality of

forage produced or still in the field.

Thus, this study aimed to evaluate the quality attributes of Tifton 85 (*Cynodon* spp.) grass using digital images obtained in the visible (RGB) and near-infrared (NIR) spectral regions, relating spectral indices to the physical, chemical, and nutritional attributes of the crop.

MATERIAL AND METHODS

Characterization of the experimental site

The experiment was carried out in a Tifton 85 (*Cynodon* spp.) grass production area at the FenoRio Farm located on the premises of UFRRJ in Seropédica, state of Rio de Janeiro, Brazil, at the geographic coordinates 22° 47' 27.68" S and 43° 40' 49.24" W (Figure 1). The area has an average altitude of 26 m and soil classified as *Argissolo Vermelho-Amarelo distrófico típico* (Ultisol) (SANTOS et al., 2018). The climate of the region, according to Köppen's (1948) classification, is Aw, characterized by a tropical climate with a dry season.



Figure 1. Experimental area located on UFRRJ premises, in Seropédica, RJ, Brazil.

The area was subjected to a standardization cut to a height of 0.05 m from the ground before the beginning of the experiment. A manual application of fertilizer by broadcasting was also carried out in all experimental units. The proportion of fertilizer used was 25% N, 0% P, and 25% K. The proportion and dose of fertilizer were chosen based on applications from previous cultivation cycles in the experimental area. The objective of varying the fertilizer dose was to obtain different levels of nutritional and spectral responses in the experimental area.

The experimental units were arranged in a Completely Randomized Block design, consisting of 4 plots (0, 100, 200, and 300 kg ha⁻¹) of 50m² (10 x 5m²) and 4 subplots (cutting

time) of 12.5m² (5 x 2.5m²) with 3 repetitions (blocks), totaling 48 experimental units in an experimental area of 0.963 ha. Analyses were performed at 14, 28, 42, and 56 days after the standardization cut (DSC).

During the experiment, meteorological data were collected through records made available by the Embrapa Meteorological Station, located in Seropédica, state of Rio de Janeiro, to characterize the environment throughout the collection periods, during the experimental period.

As observed in Table 1, the daily maximum and minimum temperatures varied between 32 and 20 °C, respectively. Daily humidity varied between 90 and 43%. With regard to rainfall, the period was marked by little

rainfall, with the highest record observed on the day after fertilization and DSC, approximately 3.18 mm. The wind speed averaged 1.67 m s^{-1} . The highest averages of solar radiation at the collection times (between 09h00 and 12h00) were recorded at 14 and 42 DSC. Although the incidence of

greater radiation at the time of collection influences the sensitivity in recording the information contained in the images, the use of spectral indices, based on the relationship between the bands, tends to minimize the effect of variation in solar radiation.

Table 1. Meteorological data on the dates of collection of digital images.

Days of collection	Temperature	Relative humidity	Rainfall	Wind	Solar Radiation
DSC	°C	%	mm	m s^{-1}	KJ m^{-2}
0	----	----	----	----	----
14	22.18	75%	0.00	2.93	1,303.53
28	26.85	72%	0.00	4.68	635.20
42	26.73	72%	0.00	4.30	1,066.60
56	25.03	75%	0.00	5.25	259.35

Digital images acquisition and processing

The experimental apparatus (Figure 2A) consisted of tripods, articulated arms, and cameras, used for image acquisition in each experimental unit (Figure 2B to Figure 2E). The articulated arms were mounted perpendicular to the ground at a distance of 1.5m. There were two digital cameras,

individually coupled to an experimental apparatus. The RGB camera, Canon S100, showed acquisition capacity at the wavelengths in the blue (450 – 495 nm), green (495 – 570 nm), and red (620 – 750 nm) bands. The RGNIR camera, Mapir Survey 3, had acquisition capacity in the green (495 – 570 nm), red (620 – 750 nm), and near-infrared (700 – 1200 nm) bands.

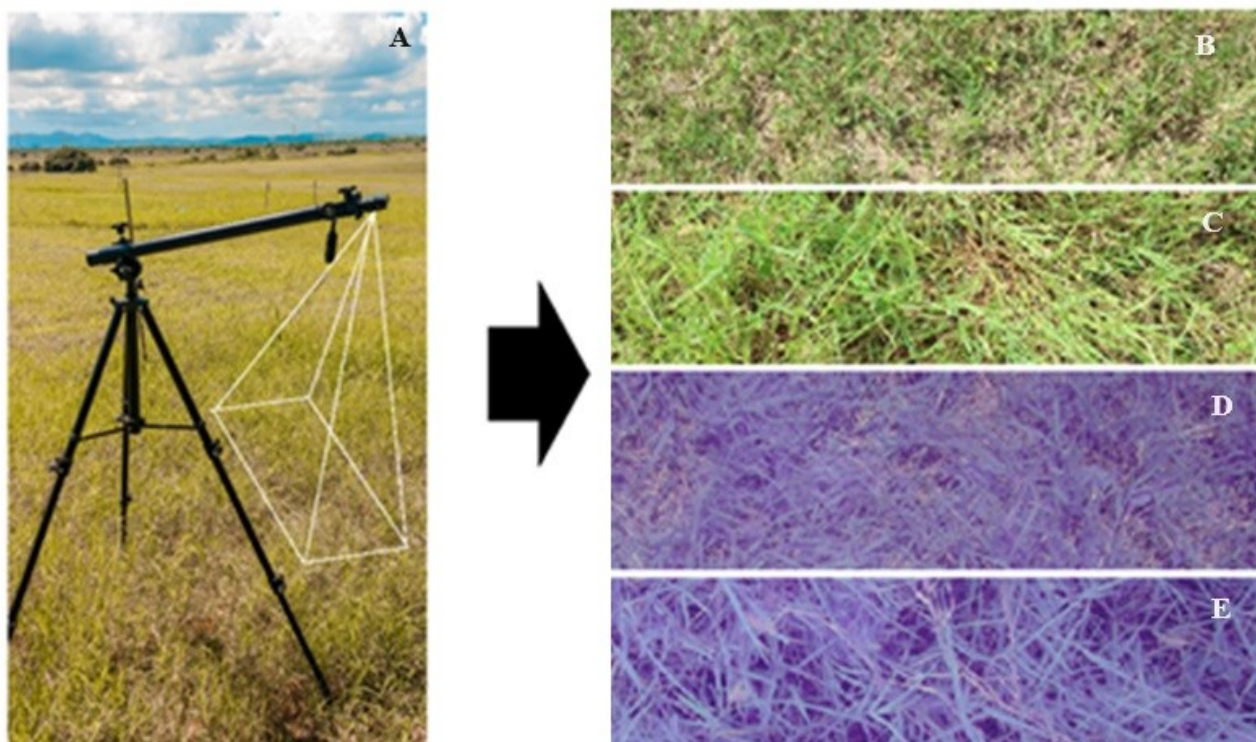


Figure 2. (A) Experimental apparatus and images generated by the RGB and RGNIR cameras: (B) Image captured with the RGB camera at 14 DSC; (C) Image captured with the RGB camera at 56 DSC; (D) Image captured with the RGNIR camera at 14 DSC and; (E) Image captured with the RGNIR camera at 56 DSC.

The RGB camera was configured to capture images with a resolution of 3648x2432 pixels, ISO1600, and automatic white balance. The RGNIR camera was configured to capture images with a resolution of 4000x3000 pixels, ISO200, and automatic white balance. The RGB images were

cropped to 5472x812 pixels and the RGNIR images to 4000x1460 pixels, to enhance the region of interest (ROI). The intensities associated with each image represented the average intensity of each band that composed the images. The average intensity values of the RGB and RGNIR images were

obtained in a computational routine developed in Python 3.10. The program was developed specifically for this study. From the average intensities of the RGB and RGNIR images, spectral indices were calculated (Table 2). These spectral indices were selected because they are consolidated indices in

the literature (FORMAGGIO; SANCHES, 2017) and are able to relate to different biophysical attributes of crops, even when using only the RGB bands collected in the visible spectral region (SENA JÚNIOR et al., 2008).

Table 2. Spectral indices calculated from images in the visible (RGB) and near-infrared (RGNIR) regions (FORMAGGIO; SANCHES, 2017; SENA JÚNIOR et al., 2008).

Spectral indice	Equation
Spectral indices obtained from RGB images	
Plant Pigment Ratio	$PPR = (G - B) / (G + B)$
Normalized Green-Red Difference	$NGRDI = (G - R) / (G + R)$
Green-red simple ratio	$GR = G/R$
Normalized excess green	$EVD = (2G-R-B)/(R+G+B)$
Spectral indices obtained from RGNIR images	
Normalized Difference Index	$NDVI_r = (NIR - R) / (NIR + R)$
Green Normalized Difference Index	$NDVI_g = (NIR - G) / (NIR + G)$
Red - near infrared ratio	$RNIR = R / NIR$
Green - near infrared ratio	$GNIR = G / NIR$
Enhanced vegetation index	$EVI = (NIR-R)/[NIR+(6R)-(7,5B)+1]$
Vegetation Index	$RATIO = NIR / R$
Transformed Vegetation Index	$TVI = \sqrt{[(NIR - R) / (NIR + R)]+0.5}$
Normalized Ratio Vegetation Index	$NRVI = (RNIR - 1)/(RNIR + 1)$

R = red band; G = green band; B = blue band; NIR = near-infrared.

Tifton 85 quality parameters

From the dry matter collected in each experimental unit at the different cutting times, the quality parameters of mineral matter, crude protein, and neutral detergent fiber were measured.

To obtain dry matter, 10 single samples were collected at random points within each experimental unit. The single samples were homogenized forming a composite sample of 0.5 kg of the same level of fertilization. For each collection period (14, 26, 42, 56 DSC), 9 repetitions of forage accumulation were obtained for each fertilization level.

The composite samples were dried in a forced air oven at 55 °C for 72 h. After drying, samples were weighed, crushed in a Wiley mill, and passed through 1.00-mm-mesh sieves. From the dry matter, the quality parameters of mineral matter, crude protein, and neutral detergent fiber were measured following the methodology of Detmann et al. (2012).

Forage accumulation (kg ha⁻¹) and forage accumulation rate (kg ha⁻¹ day⁻¹) of Tifton 85 grass were evaluated for each fertilization level over the days. The accumulation rate was given per day, and the values found at each cutting age were divided by the number of days until collection, according to Equation 1.

$$FAR = \frac{FA}{Days} \quad (1)$$

Where,

FAR - Forage accumulation rate of Tifton 85 grass (kg ha⁻¹ day⁻¹);

FA - Forage accumulation on the collection day (kg ha⁻¹); and Days - Days refer to dry matter collection days.

Data analysis

For each fertilization level (0, 100, 200, and 300 kg ha⁻¹), 5 RGB images and 5 RGNIR images were used, totaling 20 images for each cutting time (14, 28, 42, and 56 DSC).

Principal Component Analysis (PCA) was run using the PAST - Paleontological Statistics software version 4.03 (HAMMER; HARPER; RYAN, 2001) to extract the most relevant spectral indices and reduce the set of information from the original data matrix. The sets of spectral indices generated by RGB and RGNIR images were evaluated separately.

For each set of indices, the explanatory percentage and cumulative explanatory percentage of each principal component (PC) were evaluated. The correlation of spectral indices with each PC generated by RGB and RGNIR images was evaluated.

The PCs with the highest representative power (PC1) and that showed more than 70% explanatory power of the data variance were selected to evaluate the ability of the spectral indices to relate to forage quality parameters through simple quadratic regression models. The quality of the regression was evaluated by the coefficient of determination (R²).

Coefficients (scores) associated with spectral indices that did not predominantly correlate with PC1 were discarded.

This procedure generated a new principal component, called adjusted PC1. The adjusted PC1 scores were also related to the values of forage quality parameters. Figure 3 illustrates a

schematic sketch of the steps taken between obtaining the images and analyzing the relationship between the spectral indices and the quality parameters of Tifton 85.

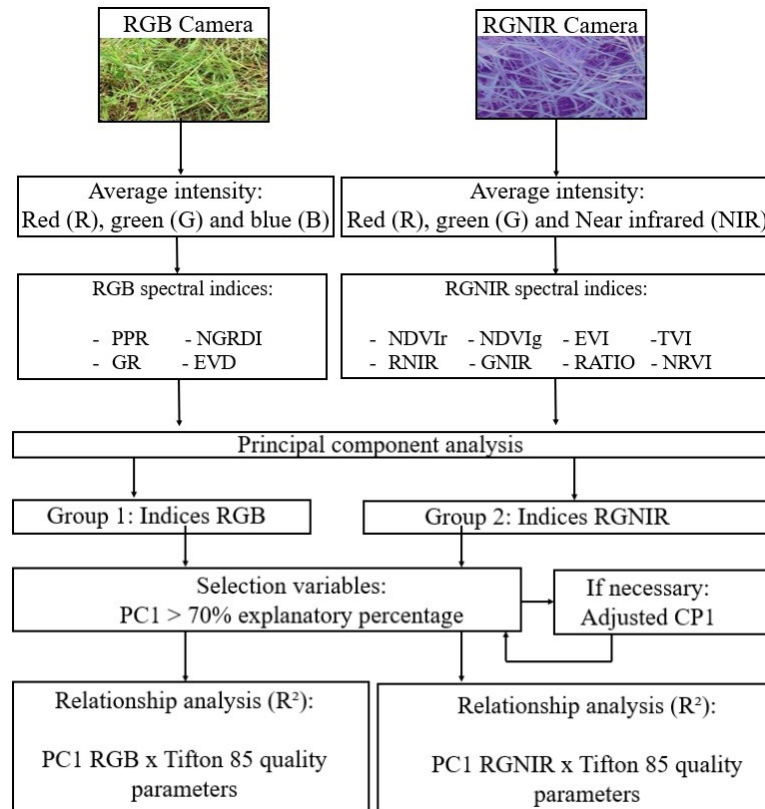


Figure 3. Steps taken between image processing and obtaining the relationship between the PC1 of spectral indices and the quality parameters of Tifton 85.

RESULTS AND DISCUSSION

Characterization of Tifton 85 development during the experiment

For the forage accumulation of Tifton 85 (Figure 4A), the effect of fertilization was observed throughout all collection days. Lower forage accumulations were found in areas that did not receive fertilizer, while the highest values

were observed with nitrogen fertilization at 300 kg ha⁻¹. The analysis of the forage accumulation rate of Tifton 85 (Figure 4B) grass after the standardization cut (DSC) indicated that the highest forage accumulation occurred at 42 DSC in the experimental units that received the fertilizer dose of 300 kg ha⁻¹. At 56 DSC, there was a reduction in the forage accumulation rate, which indicates that at this moment the forage already showed a decrease in vigor, which may affect biophysical and nutritional parameters.

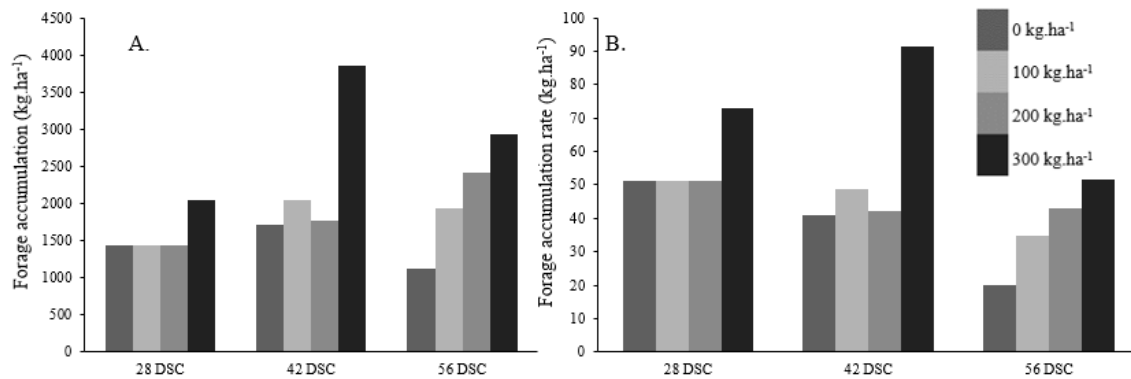


Figure 4. (A) Forage accumulation (kg ha⁻¹) and (B) forage accumulation rate (kg ha⁻¹) of Tifton 85 grass at 28, 42, and 56 days after standardization cut (DSC) as a function of fertilization levels.

Some studies on Tifton 85 showed results similar to those observed in Figure 4 for the increase in forage production from nitrogen fertilization. Delongui and Coelho (2018) obtained the highest levels of forage production related to nitrogen fertilization at 300 and 400 kg ha⁻¹. Schaeffer et al. (2021) demonstrated that nitrogen fertilization at 100 and 200 kg ha⁻¹ already allows a significant increase in Tifton 85 production compared to areas without this type of fertilization. Andrade et al. (2018) found that hay produced from Tifton 85 fertilized with 300 kg ha⁻¹ nitrogen and harvested within 37 days resulted in higher dry matter production. Patzlaff et al. (2020) concluded that doses of approximately 400 kg ha⁻¹ allowed greater production of green mass, dry mass, and a higher forage accumulation rate for Tifton 85, compared to doses of 200 kg ha⁻¹.

Relationship between spectral indices and quality parameters of Tifton 85

The analysis of the explanatory percentage (EP) and cumulative explanatory percentage (CEP) of the PCs, generated from the sets of spectral indices obtained by RGB and RGNIR images is presented in Table 3. EP allows evaluating the percentage of variance in the dataset explained by each component, while CEP enables assessment of the

accumulated percentage of variance in the sum of the components. Results demonstrated that the indices obtained by RGB images at the 28 DSC cutting age had the highest explanatory percentage (EP = 94.10%) associated with PC1, while the indices obtained by RGNIR images had the highest explanatory percentage (EP = 93.44%) associated with PC1 at the 42 DSC cutting age. The spectral indices associated with the other times had the variance predominantly explained by PC1 (CEP > 70%), except the times 42 DSC for RGB images and 56 DSC for RGNIR images, indicating that it was possible to reduce the set to one component for the total RGB and RGNIR spectral indices.

The correlation between the RGB and RGNIR spectral indices and the most relevant PCs for each cutting time (Table 4) allowed assessing which indices were influential in obtaining the PC1 scores. This evaluation made it possible to eliminate the indices that showed a low correlation with PC1, aiming to increase the explanatory power of this PC for cutting times at which the EP was less than 70%. Thus, for the adjustment of the equation associated with PC1 (adjusted PC1), the PPR and EVD indices obtained in RGB images at the time of 42 DSC were discarded. Similarly, the NDVIg and GNIR indices obtained in the RGNIR images at 56 DSC were discarded, generating an adjustment of the equation associated with PC1 at these times.

Table 3. Explanatory percentage (EP) and cumulative explanatory percentage (CEP) of the principal components generated by the RGB and RGNIR indices for each evaluated age.

	RGB Images		RGNIR Images		
	PC1	PC2	PC1	PC2	
	14 days		14 days		
EP (%)	90.89	09.10	EP (%)	95.58	04.35
CEP (%)	90.89	99.99	CEP (%)	95.58	99.93
Eigenvector	0.019	0.002	Eigenvector	0.033	0.001
	28 days		28 days		
EP (%)	94.10	05.90	EP (%)	89.18	10.78
CEP (%)	94.10	99.99	CEP (%)	89.18	99.96
Eigenvector	0.003	0.000	Eigenvector	0.004	0.001
	42 days		42 days		
EP (%)	56.38	43.61	EP (%)	93.44	06.40
CEP (%)	56.38	99.99	CEP (%)	93.44	99.84
Eigenvector	0.006	0.004	Eigenvector	0.029	0.002
	56 days		56 days		
EP (%)	76.45	23.55	EP (%)	60.22	39.77
CEP (%)	76.45	99.99	CEP (%)	60.22	99.99
Eigenvector	0.002	0.000	Eigenvector	0.002	0.001

Table 4. Correlation between the principal components (PC) of greater relevance and the spectral indices associated with RGB and RGNIR images at each cutting time (days after the standardization cut - DSC).

	14 DSC		28 DSC		42 DSC		56 DSC	
	PC1	PC2	PC1	PC2	PC1	PC2	PC1	PC2
Indices associated with RGB images								
PPR	0.23	0.97	0.89	0.46	-0.50	0.87	0.26	0.97
NGRDI	0.99	-0.06	0.98	-0.17	0.96	0.28	0.98	-0.19
GR	0.99	-0.08	0.98	-0.18	0.97	0.25	0.98	-0.18
EVD	0.91	0.41	0.99	0.14	0.09	0.99	0.88	0.48
Indices associated with RGNIR images								
NDV _{Ir}	0.99	0.16	0.97	0.23	0.99	0.10	-0.01	0.99
NDV _{Ig}	0.97	-0.26	0.89	-0.46	0.81	-0.58	-0.99	0.01
RNIR	-0.99	-0.15	-0.97	-0.23	-0.99	-0.09	0.01	0.99
GNIR	-0.97	0.25	-0.89	0.46	-0.82	0.57	0.99	0.01
EVI	0.98	0.18	0.97	0.23	0.99	0.10	-0.01	0.99
RATIO	0.98	0.19	0.97	0.24	0.99	0.10	-0.01	0.99
TVI	0.99	0.16	0.98	0.23	0.99	0.09	-0.01	0.99
NRVI	-0.99	-0.16	-0.97	-0.23	-0.99	-0.10	0.01	-0.99

PPR = Plant Pigment Ratio; NGRDI = Normalized Green-Red Difference; GR = Green-red simple ratio; EVD = Normalized excess green; NDV_{Ir} = Normalized Difference Index; NDV_{Ig} = Green Normalized Difference Index; RNIR = Red - near infrared ratio; GNIR = Green - near infrared ratio; EVI = Enhanced vegetation index; RATIO = Vegetation Index; TVI = Transformed Vegetation Index; NRVI = Normalized Ratio Vegetation Index.

After removing the spectral indices that were correlated with PC2, the coefficients associated with PC1 that had explanatory power greater than 70% were obtained. The adjusted PC1 coefficients represented the spectral indices with greater weight in the calculation of scores for this PC.

Table 5 lists the coefficients associated with spectral indices of RGB and RNIR images, which were used in the equation for calculating PC1. In relation to the spectral indices obtained by RGB images, the GR index showed higher

coefficients, indicating that it has a greater influence on the calculation of PC1 at all evaluated cutting times. Regarding the spectral indices obtained by the RGNIR images, at 14 DSC and 28 DSC, the GNIR and RATIO indices, which relate the G and R bands, respectively, with the band in the near-infrared region, most influenced the calculation of PC1. At 42 DSC, the indices with the highest weights were RNIR and RATIO, while at 56 DSC, EVI, RATIO, and NRVI indices had a greater influence on PC1.

Table 5. Coefficients used to calculate the PC1 from spectral indices generated by RGB and RGNIR images.

RGB Images - Coefficients associated with PC1								
$PC1 = (a_1 * PPR) + (a_2 * NGRDI) + (a_3 * GR) + (a_4 * EVD)$								
	PPR (a ₁)	NGRDI (a ₂)	GR (a ₃)	EVD (a ₄)				
14 DSC	0.063	0.369	0.864	0.338				
28 DSC	0.372	0.310	0.717	0.502				
42 DSC	*	0.387	0.922	*				
56 DSC	0.129	0.366	0.826	0.409				
RGNIR Images - Coefficients associated with PC1								
$PC1 = (a_1 * NDV_{Ir}) + (a_2 * NDV_{Ig}) + (a_3 * RNIR) + (a_4 * GNIR) + (a_5 * EVI) + (a_6 * RATIO) + (a_7 * TVI) + (a_8 * NRVI)$								
	NDV _{Ir} (a ₁)	NDV _{Ig} (a ₂)	RNIR (a ₃)	GNIR (a ₄)	EVI (a ₅)	RATIO (a ₆)	TVI (a ₇)	NRVI (a ₈)
14 DSC	0.230	0.343	-0.390	-0.534	0.075	0.558	0.150	-0.230
28 DSC	0.239	0.333	-0.372	-0.448	0.084	0.638	0.150	-0.239
42 DSC	0.276	0.199	-0.453	-0.285	0.092	0.694	0.177	-0.276
56 DSC	0.249	*	0.342	*	-0.426	-0.534	0.077	0.590

* - spectral indices removed to obtain the adjusted PC1. DSC = Days after the standardization cut.

In forage crops, modeling methods based on spectral characteristics have been applied with the objective of monitoring and estimating the physical and chemical parameters of forages. Nilsson et al. (2023) also evaluated *Urochloa brizantha* cv. Marandu using the NDVI index, as a function of nitrogen fertilization levels, and obtained significant linear relationships between data and characteristics of the crop canopy. Tong et al. (2019) used the spectral indices SRVI, NDVI, SAVI, and EVI to evaluate the predictive performance of stepwise multiple linear regression (SMLR) in estimating pasture biomass. In these cases, although the spectral indices showed satisfactory relationships with the physical and chemical attributes of the crops, the relationship with the nutritional parameters of the crop was not studied.

Once the PC1 values for each DSC and each fertilization level were obtained, the relationships between the spectral indices represented by the PC1 and the quality parameters of Tifton 85 grass were analyzed. The purpose of this evaluation was to observe which times were the most suitable for applying models based on information obtained

by digital images to estimate the quality parameters of crude protein (CP), mineral matter (MM), and neutral detergent fiber (NDF).

The quadratic relationships between the quality parameters of Tifton 85 obtained at different fertilization levels and the PC1, generated by spectral indices obtained by RGB images, are listed in Table 6. When analyzing the spectral indices and PC1, the highest relationships between spectral indices and quality parameters occurred at 42 DSC for MM ($R^2 = 0.83$), at 28 DSC for CP ($R^2 = 0.94$), and at 14 DSC for NDF ($R^2 = 0.96$). These ages are the most suitable times for estimating the quality parameters of Tifton 85 from digital images. NDF was the parameter that indicated the possibility of estimation by earlier digital RGB images since high relationships were found at the initial cutting times. On the other hand, despite the high relationship observed at 42 DSC, the MM showed a low relationship with the spectral indices ($R^2 < 0.50$) at the other cutting times, which indicates that the spectral indices used may have limitations for estimating this attribute.

Table 6. Equations fit for the quadratic relationship between the Tifton 85 quality parameters and the principal components 1 (PC1), generated by spectral indices obtained by RGB images on different days after the standardization cut (DSC).

Parameter	Equations fit	R ²	Indicated Time
Mineral Matter (MM)	$MM_{14DSC} = 18.22PC1^2 + 0.21PC1 + 6.26$	0.24	42 DSC
	$MM_{28DSC} = -7.24PC1^2 - 0.62PC1 + 7.23$	0.01	
	$MM_{42DSC} = -256.40PC1^2 - 14.19PC1 + 6.96$	0.83	
	$MM_{56DSC} = 252.90PC1^2 + 4.14PC1 + 6.23$	0.49	
Crude Protein (CP)	$CP_{14DSC} = -40.91PC1^2 + 9.04PC1 + 9.42$	0.85	28 DSC
	$CP_{28DSC} = -903.67PC1^2 + 2.14PC1 + 9.57$	0.94	
	$CP_{42DSC} = -137.07PC1^2 - 2.56PC1 + 7.31$	0.60	
	$CP_{56DSC} = 240.11PC1^2 - 5.10PC1 + 6.44$	0.82	
Neutral detergent fiber (NDF)	$NDF_{14DSC} = 72.24PC1^2 - 11.48PC1 + 76.20$	0.96	14 DSC
	$NDF_{28DSC} = -2237PC1^2 + 9.53PC1 + 81.47$	0.86	
	$NDF_{42DSC} = 853.60PC1^2 + 42.85PC1 + 78.74$	0.45	
	$NDF_{56DSC} = -1573PC1^2 + 7.97PC1 + 85.75$	0.19	

As for the relationship between the quality parameters and the spectral indices obtained by RGNIR images (Table 7), in general, these variables were more related at the evaluated times. The highest relationships were obtained at 42 DSC for MM ($R^2 = 0.99$), at 14 DSC for CP ($R^2 = 0.88$), and at 42 DSC for NDF ($R^2 = 0.99$). Except for MM, all the quality parameters showed a relationship greater than $R^2 = 0.80$ with the spectral indices, demonstrating that, in general, the use of RGNIR images enables an earlier evaluation of quality parameters compared to the results obtained by RGB images. As for the MM, even with an increase in the coefficients of determination from RGNIR images, the relationships with

spectral indices continued to be predominantly discreet, reinforcing the indication of limitations for estimating this attribute from digital images.

Based on the results in Table 6 and Table 7, in general, RGNIR images are the most suitable for obtaining information on the quality of Tifton 85 at early times. However, because an RGB camera is a lower cost device compared to an RGNIR camera, the use of RGB images is more indicated for evaluating quality parameters that obtained high relationships with spectral indices both for the RGB and the RGNIR images, as well as in the case of CP and NDF.

Table 7. Equations fit for the quadratic relationship between the Tifton 85 quality parameters and the principal components 1 (PC1), generated by spectral indices obtained by RGNIR images on different days after the standardization cut (DSC).

Parameter	Equations fit	R ²	Indicated Time
Mineral Matter (MM)	$MM_{14DSC} = 10.49PC1^2 - 1.53PC1 + 6.78$	0.66	42 DSC
	$MM_{28DSC} = -215.09PC1^2 - 10.03PC1 + 7.51$	0.76	
	$MM_{42DSC} = 12.53PC1^2 + 2.34PC1 + 6.24$	0.99	
	$MM_{56DSC} = 1.41PC1^2 - 0.26PC1 + 6.32$	0.05	
Crude Protein (CP)	$CP_{14DSC} = -11.96PC1^2 + 4.18PC1 + 9.23$	0.88	14 DSC
	$CP_{28DSC} = 44.97PC1^2 + 12.12PC1 + 8.93$	0.82	
	$CP_{42DSC} = 35.04PC1^2 - 1.88PC1 + 6.63$	0.75	
	$CP_{56DSC} = 15.48PC1^2 - 0.02PC1 + 6.25$	0.84	
Neutral detergent fiber (NDF)	$NDF_{14DSC} = -26.29PC1^2 - 10.99PC1 + 77.85$	0.96	42 DSC
	$NDF_{28DSC} = 198.48PC1^2 + 36.87PC1 + 79.73$	0.92	
	$NDF_{42DSC} = -94.49PC1^2 - 9.90PC1 + 81.70$	0.99	
	$NDF_{56DSC} = 2.90PC1^2 + 8.76PC1 + 85.01$	0.54	

Our findings reinforce the potential of using image-based technologies to monitor the nutritional and chemical quality of Tifton 85 in the field and can help in decision-making regarding the management of forage crops (SUNOJ et al., 2021). The low-cost, easy-to-handle, non-invasive technology, with faster measurement than traditional laboratory analysis, can drive the development of alternative methods of sampling in the field.

Observing the relationship between spectral indices and crop quality parameters makes it possible to advance studies in this field of research, based on the generation of estimation models complementary to laboratory analyses, contributing to meeting the demand for new technologies applicable to the farming sector.

CONCLUSION

The application of principal component analysis allowed summarizing the information given by spectral indices obtained by digital RGB and RGNIR images into the first principal component (PC1) at all cutting times of Tifton 85. The PC1 associated with the indices obtained by RGB images had the highest explanatory power (EP = 94.10%) at 28 DSC, while PC1 associated with indices obtained by RGNIR images had the highest explanatory power (EP = 93.44%) at 42 DSC.

The analysis of the relationship between spectral indices obtained by RGB images and the quality parameters of Tifton 85 demonstrated that NDF (R² = 0.96) and CP (R² = 0.94) had the highest relationships with spectral indices at 14 DSC and 28 DSC, respectively. These ages were considered the most suitable for the analysis of these parameters from RGB images.

Compared to results obtained from RGB images, the spectral indices obtained from RGNIR images predominantly showed a greater relationship with the Tifton 85 quality parameters. CP and NDF showed a high relationship with spectral indices already at earlier times, demonstrating that although the RGB images show satisfactory results, RGNIR images are the most indicated to obtain information on the quality of Tifton 85 grass at early times. As for MM, the

relationships with spectral indices obtained by RGB and RGNIR images proved to be variable over time, indicating limitations for estimating this attribute from digital images.

ACKNOWLEDGMENTS

The authors would like to thank the Coordination for the Improvement of Higher Education Personnel (CAPES) and the Carlos Chagas Filho Foundation for Research Support in the State of Rio de Janeiro (FAPERJ).

REFERENCES

- AHMAD, N. et al. The effects of technological innovation on sustainable development and environmental degradation: Evidence from China. **Technology in Society**, 72: 102184, 2023.
- ANDRADE, W. R. et al. Hay Tifton-85 grass under nitrogen doses in different days of regrowth. **Acta Scientiarum Animal Sciences**, 40: 37692, 2018.
- DELONGUI, R.; COALHO, M. R. Avaliação das características morfológicas sobre a produção e composição bromatológica do Capim-Tifton 85 submetido a diferentes doses de nitrogênio. **Revista Terra & Cultura: Cadernos de Ensino e Pesquisa**, 34: 64 -73, 2018.
- DETMANN, E. et al. **Métodos para análise de alimentos**. 1. ed. Visconde do Rio Branco, MG: Suprema, 2012. 214 p.
- EMBRAPA - Empresa Brasileira de Pesquisa Agropecuária. **Monitoramento tecnológico de cultivares de forragens no Brasil**. São Carlos, SP: Embrapa Pecuária Sudeste, 2021. 34 p. (Documentos, 139.)
- FAO - Food and Agriculture Organization of the United Nations. **Alimentos e Agricultura no mundo: Anuário Estatístico**. Roma: FAO, 2022. 382 p.

- FORMAGGIO, A. R.; SANCHES, L. D. **Sensoriamento remoto em agricultura**. 1. ed. São Paulo, SP: Oficina do texto, 2017. 288 p.
- HAMMER, O.; HARPER, D. A. T.; RYAN, P. D. PAST - Paleontological Statistics software package for education and data analysis. **Palaentologia Eletrônica**, 4: 1-9, 2001.
- HUACCHA-CASTILLO, A. E. et al. Non-destructive estimation of leaf area and leaf weight of *Cinchona officinalis* L.(*Rubiaceae*) based on linear models. **Forest Science and Technology**, 19: 59-67, 2023.
- KŘÍŽOVÁ, K. et al. Using a single-board computer as a low-cost instrument for SPAD value estimation through colour images and chlorophyll-related spectral indices. **Ecological Informatics**, 67: 101496, 2022.
- KÖPPEN, W. **Climatologia: con un estudio de los climas de la tierra**. Fondo de Cultura Econômica. 1948, 479 p.
- MAIMAITIJIANG, M. et al. Vegetation Index Weighted Canopy Volume Model (CVMVI) for soybean biomass estimation from Unmanned Aerial System-based RGB imagery. **ISPRS Journal of Photogrammetry and Remote Sensing**, 151: 27-41, 2019.
- MANCIN, W. R. et al. The use of computer vision to classify Xaraés grass according to nutritional status in nitrogen. **Revista Ciência Agronômica**, 53: 20207797, 2022.
- NILSSON, M. S. et al. Effect of different nitrogen fertilization rates on the spectral response of *Brachiaria brizantha* cv. Marandú leaves. **Engenharia Agrícola**, 43: e20220008, 2023.
- PATZLAFF, N. L. et al. A importância do uso da dose correta na adubação nitrogenada de tifton 85. **Revista Científica Rural**, 22: 1-12, 2020.
- PETERS, K. C. et al. Field-scale calibration of the PAR Ceptometer and FieldScout CM for real-time estimation of herbage mass and nutritive value of rotationally grazed tropical pasture. **Smart Agricultural Technology**, 2: 100037, 2022.
- SANTOS, H. G. et al. **Sistema Brasileiro de Classificação de Solos**. 5. ed. Brasília, DF: Embrapa, 2018. 356 p.
- SCHAEFFER, G. H. et al. Avaliação do desenvolvimento de grama tifton 85 submetida a diferentes doses e fontes de nitrogênio. **Anuário Pesquisa e Extensão Unoesc São Miguel do Oeste**, 6: 27735, 2021.
- SENA JÚNIOR, D. G. et al. Discriminação entre estágios nutricionais na cultura do trigo com técnicas de visão artificial e medidor portátil de clorofila. **Revista de Engenharia Agrícola**, 28: 187-195, 2008.
- SERRET, M. D. et al. Vegetation indices derived from digital images and stable carbon and nitrogen isotope signatures as indicators of date palm performance under salinity. **Agricultural Water Management**, 230: 105949, 2020.
- SILVA, C. J. A. et al. How lamb production systems can affect the characteristics and sward structure of Tifton 85 pasture?. **Small Ruminant Research**, 188: 106124, 2020.
- SOMAVILLA, A. et al. Chemical pattern of vegetation and topsoil of rangeland fertilized over 21 years with phosphorus sources and limestone. **Soil and Tillage Research**, 205: 104759, 2021.
- SUNOJ, S. et al. Digital image analysis estimates of biomass, carbon, and nitrogen uptake of winter cereal cover crops. **Computers and Electronics in Agriculture**, 184: 106093, 2021.
- SOUZA, C. D. et al. Natural Genetic Diversity of Nutritive Value Traits in the Genus *Cynodon*. **Agronomy**, 10: 1729, 2020.
- TONG, X. et al. Combined use of in situ hyperspectral vegetation indices for estimating pasture biomass at peak productive period for harvest decision. **Precision Agriculture**, 20: 477-495, 2019.
- WANG, H. et al. Regulation of Density and Fertilization on Crude Protein Synthesis in Forage Maize in a Semiarid Rain-Fed Area. **Agriculture**, 13: 715, 2023.